The American Journal of Pathology, Vol. 181, No. 3, September 2012

http://dx.doi.org/10.1016/j.ajpath.2012.05.016

Molecular Pathogenesis of Genetic and Inherited Diseases

Myotubularin-Deficient Myoblasts Display Increased Apoptosis, Delayed Proliferation, and Poor Cell Engraftment

Michael W. Lawlor,*† Matthew S. Alexander,* Marissa G. Viola,* Hui Meng,† Romain Joubert,‡ Vandana Gupta,* Norio Motohashi,* Richard A. Manfready,* Cynthia P. Hsu,* Ping Huang,* Anna Buj-Bello,‡ Louis M. Kunkel,* Alan H. Beggs,* and Emanuela Gussoni*

From the Division of Genetics and the Program in Genomics, The Manton Center for Orphan Disease Research, Children's Hospital Boston, Harvard Medical School, Boston, Massachusetts; the Division of Pediatric Pathology, the Department of Pathology and Laboratory Medicine,† Medical College of Wisconsin, Milwaukee, Wisconsin; and the Department of Research and Development,‡ Genethon, INSERM, Evry, France*

X-linked myotubular myopathy is a severe congenital myopathy caused by deficiency of the lipid phosphatase, myotubularin. Recent studies of human tissue and animal models have discovered structural and physiological abnormalities in myotubularin-deficient muscle, but the impact of myotubularin deficiency on myogenic stem cells within muscles is unclear. In the present study, we evaluated the viability, proliferative capacity, and *in vivo* engraftment of myogenic cells obtained from severely symptomatic (*Mtm1*δ4) myotubularin-deficient mice. *Mtm1*δ4 muscle contains fewer myogenic cells than wild-type (WT) littermates, and the number of myogenic cells decreases with age. The behavior of *Mtm1*δ4 myoblasts is also abnormal, because they engraft poorly into C57BL/6/Rag1null/mdx5cv mice and display decreased proliferation and increased apoptosis compared with WT myoblasts. Evaluation of *Mtm1*δ4 animals at 21 and 42 days of life detected fewer satellite cells in *Mtm1*δ4 muscle compared with WT littermates, and the decrease in satellite cells correlated with progression of disease. In addition, analysis of WT and *Mtm1*δ4 regeneration after injury detected similar abnormalities of satellite cell function, with fewer satellite cells, fewer dividing cells, and increased apoptotic cells in *Mtm1*δ4 muscle. These studies demonstrate specific abnormalities in myogenic cell number and behavior that may relate to the progression of disease in myotubularin deficiency, and may also be used to develop *in vitro* assays by which novel treatment strategies can be assessed. (*Am J Pathol 2012, 181:961–968; http://dx.doi.org/10.1016/j.ajpath.2012.05.016*)

X-linked myotubular myopathy (XLMTM) is a severe form of congenital myopathy with an estimated incidence of 1:50,000 male births that most often presents with severe perinatal weakness and respiratory failure.[1–3] XLMTM is caused by mutations in the *MTM1* gene that encodes a phosphoinositide phosphatase called myotubularin. Myotubularin plays a role in multiple cellular processes, including endosomal trafficking,[4] excitation contraction coupling,[5–7] intermediate filament organization,[8] and apoptosis.[9] Muscle biopsy specimens from patients with XLMTM display excessively small fibers with increased numbers of central nuclei and aggregation of organelles within the central regions of many cells.[3] A murine model of myotubularin deficiency, the *Mtm1*δ4 mouse [also referred to as *Mtm1* knock-

Supported by the NIH (P50 NS040828, R01 AR044345, K08 AR059750, and R01NS047727; Loan Repayment Program L40 AR057721), the Muscular Dystrophy Association (United States) (MDA201302), the Joshua Frase Foundation, the Lee and Penny Anderson Family Foundation, the French Association Against Myopathy, the Myotubular Trust (United Kingdom), the ATIGE-Genopole d'Evry (France), and the American Heart Association (SDG 0730285N).

Accepted for publication May 22, 2012.

Disclosures: FACS was performed in the Intellectual and Developmental Disabilities Research Center Stem Cell Core Facility at Children's Hospital Boston, supported by an award from the NIH (NIH-P30-HD18655). The Pax7 antibody was obtained from the Developmental Studies Hybridoma Bank at the University of Iowa, developed under the auspices of the Eunice Kennedy Shriver National Institute of Child Heath & Human Development.

Current address of M.W.L., Department of Pathology and Laboratory Medicine, Children's Hospital of Wisconsin and Medical College of Wisconsin, Milwaukee, Wisconsin.

Address reprint requests to Alan H. Beggs, Ph.D., Genetics Division, CLSB 15026, or Emanuela Gussoni, Ph.D., Genetics Division, Center for Life Sciences, Boston, 15021, Children's Hospital Boston, 300 Longwood Ave, Boston, MA 02115. E-mail: beggs@enders.tch.harvard.edu or gussoni@enders.tch.harvard.edu.

out (KO) in prior studies[5,7,10,11]], shows similar features to the human disease, including severe weakness, respiratory failure, and histological findings that include myofiber smallness and increased numbers of centrally nucleated fibers.[11] Whether the myofiber smallness might be due to poor function of satellite cells and/or other myogenic progenitors remains unclear.

To identify whether there was an easily testable phenotype in myotubularin-deficient myoblasts, we used fluorescence-activated cell sorting (FACS) to isolate prospective myogenic cell fractions from *Mtm1*δ4 and wild-type (WT) animals and assessed proliferation, apoptosis, fusion, and engraftment of these cells. Muscle from 25- to 30-day-old *Mtm1*δ4 mice had a consistently increased number of cells in the stem cell antigen (SCA)1$^-$, CD45$^-$, platelet-derived growth factor receptor (PDGFR) α^-, and propidium iodide$^-$ (quadruple-negative) population compared with their WT littermates. In contrast, the number of CD31$^-$, CD45$^-$, CD106$^+$ [vascular cell adhesion molecule 1 (VCAM1$^+$)] myogenic cells, and evaluations of Pax7 expression, revealed decreased numbers of satellite cells in *Mtm1*δ4 mice that progressed with age. *Mtm1*δ4 myoblasts also displayed increased apoptosis, slow proliferation, and poor engraftment compared with WT myoblasts. This corresponded to increased apoptosis, decreased proliferation, and reduced numbers of Pax7$^+$ satellite cells after cardiotoxin injection, as well as a progressive decrease in the number of Pax7$^+$ satellite cells with the progression of disease, in *Mtm1*δ4 mice. These functional abnormalities in myogenic cells can partially explain the inevitable decline of *Mtm1*δ4 muscles, and they provide reproducible and potentially testable biomarkers for myotubularin deficiency in this cell population.

Materials and Methods

Animals

All studies were fully approved by the Institutional Animal Care and Use Committee at Children's Hospital Boston (Boston, MA). Mtm1/C57BL/6 (*Mtm1*δ4) mice were bred and genotyped as previously described.[12] Cell transplantation studies used dystrophin-deficient 5- to 6-month-old immunocompromised C57BL/6 Rag1null *mdx*5cv mice, which were custom generated at the Jackson Laboratory (Bar Harbor, ME) by crossing mdx5cv mice with Rag1-null mice.

Myoblast Isolation and FACS

Quadruple-Negative Cells

Primary muscle cells were dissected and dissociated in parallel from the upper and lower limbs of *Mtm1*δ4 and WT littermate mice between 25 and 30 days of life (DOL) following established methods.[13,14] Cells were incubated on ice with fluorescein isothiocyanate–conjugated anti-Ly-6A/E (SCA-1, clone E13-161.7; BD Biosciences, San Jose, CA), phosphatidylethanolamine-Cy5–conjugated anti-CD45 (clone 30F11; BD Biosciences), and APC-conjugated anti-CD140a (PDGFRα, clone APA5; BioLegend, San Diego, CA) antibodies and propidium iodide (Sigma Aldrich, St Louis, MO) for 45 minutes. Cells were then analyzed and sorted using a BD FACS Aria cell sorter to isolate the SCA1$^-$CD45$^-$PDGFRα^-PI$^-$ (quadruple-negative) population.

CD31$^-$CD45$^-$VCAM$^+$ Myogenic Cells

Primary muscle cells were dissociated from *Mtm1*δ4 and WT mice at 45 to 49 DOL, as previously described. The antibodies used for FACS analysis included fluorescein isothiocyanate–conjugated anti-CD31 antibody (clone 390; BD Biosciences), phosphatidylethanolamine-conjugated anti-CD45 (clone 30-F11; BD Biosciences), and APC-conjugated CD106 (clone 429; BioLegend).

Proliferation Assays

Quadruple-negative cells from 25- to 30-day-old WT or *Mtm1*δ4 mice were plated onto 96-well plates at a density of either 1000, 5000, or 10,000 cells per well in Human Skeletal Muscle Growth Media (Promocell, Heidelberg, Germany). Proliferation was measured at 0, 2, and 4 days after isolation using a CellTiter 96 AQueous Non-Radioactive Cell Proliferation Assay (number TB169; Promega, Madison, WI), per manufacturer's instructions. Absorbance was read at 490 nm using a Synergy 2 plate reader (Biotek Instruments, Winooski, VT). The average of three wells for each condition was recorded for each time point, data were standardized by comparing the values from WT with *Mtm1*δ4 cells from each individual animal pair, and the entire experiment was repeated three times. Statistical differences between corrected values were compared using a two-way analysis of variance.

Caspase Assays

After FACS, 250,000 quadruple-negative cells from 25- to 30-day-old WT or *Mtm1*δ4 mice were plated onto a 10-cm collagen-coated culture dish in Human Skeletal Muscle Growth Media (Promocell). Three aliquots of 100,000 quadruple-negative cells were also frozen as a time = 0 condition. After 2 or 4 days in culture, three aliquots of 80,000 cells were frozen at −80°C. Apoptosis was evaluated using a Caspase-Glo 3/7 Assay kit (Promega), following the manufacturer's instructions, and read on a single-tube luminometer (Berthold Instruments, Oak Ridge, TN). Statistical differences between corrected values were compared using a two-way analysis of variance. Depending on cell yields available from each animal, between 1 and 3 replicates at each time point were performed on each animal cell isolate, using five different animal isolates for each genotype.

Fusion Assays

Primary myogenic cells from 25- to 30-day-old WT or *Mtm1*δ4 mice were enriched using the preplating technique.[15] Myogenic cells were cultured on Matrigel-coated plates in Dulbecco's modified Eagle's medium (DMEM) high glucose supplemented with 30% fetal bo-

vine serum (FBS) and 3 μg/mL basic fibroblast growth factor. For fusion assays, 10,000 cells per well were plated in eight-well permanox slides coated with Matrigel. Cells adhered overnight in high serum medium, then switched to differentiation medium (DMEM low glucose supplemented with 4% FBS). Differentiation medium was changed daily, and fusion was assessed at days 0, 2, and 5 after the induction of differentiation. Cells were fixed and stained with a rabbit monoclonal anti-desmin antibody (Epitomics) diluted 1:100. The percentage of fused cells was calculated using 10 randomly photographed fields for each animal. Data were collected from three animals per genotype. Alternatively, quadruple-negative cells from 25- to 30-day-old WT or *Mtm1*δ4 mice were plated onto gelatin in a 48-well culture plate at 50,000 cells per well in DMEM High Glucose plus 20% FBS and 3 μg/mL basic fibroblast growth factor (Invitrogen, Carlsbad, CA). Media were changed every 2 days until the cultures reached 70% confluence, and then media were changed to DMEM Low Glucose (Invitrogen) plus 2% FBS to promote differentiation. Media were changed daily for 3 days. After methanol fixation, immunohistochemical (IHC) staining was performed using standard techniques, with anti-human desmin primary antibodies (1:100, M0760; Dako, Carpentaria, CA) and AlexaFluor 568–conjugated goat anti-mouse IgG secondary antibodies (Invitrogen). Slides were coverslipped in Vectashield Hard Set mounting media containing DAPI (Vector Laboratories, Burlingame, CA) and evaluated using a Nikon TE-2000S microscope (Nikon, Melville, NY). The fusion index in control and myotubularin-deficient culture cells was calculated as the ratio of fused nuclei within myotubes/number of total nuclei. Fusion indices were compared in control and mutant cultures using the Student's *t*-test. These studies were performed using myoblasts isolated from two different mice of each genotype and two to three replicates performed per mouse, depending on cell yields.

FDB Preparations

Flexor digitorum brevis (FDB) muscles from 25- to 30-day-old WT or *Mtm1*δ4 mice were extracted using standard techniques[16,17] and plated on laminin-coated chamber slides. After incubating for 6 hours in DMEM with 10% FBS, cultured fibers were fixed in paraformaldehyde and stained for Pax7 (Developmental Studies Hybridoma Bank, Iowa City, IA) and DAPI using standard IHC techniques.[16] Data were quantified as the number of fibers containing satellite cells per 100 fibers evaluated. The number of nuclei per fiber was nearly identical when comparing WT with KO cultures within the images quantified.

Western Blot Analysis

Quadruple-negative cells were pelleted and then lysed using MPER buffer (Thermo Scientific, Waltham, MA) containing protease and phosphatase inhibitors at a concentration of 1 μL per 10,000 cells isolated. Western blot procedures were performed as previously described.[18] Transferred proteins were probed with antibodies against Pax7 (Developmental Studies Hybridoma Bank) and glyceraldehyde-3-phosphate dehydrogenase (6C5; Abcam, Cambridge, MA) and visualized using enhanced chemiluminescence. Quantification of protein levels normalized to glyceraldehyde-3-phosphate dehydrogenase was performed with the program Quantity One version 4.2.1 (Bio-Rad Laboratories), on an Image Station 440 (Kodak DS).

Pax7 mRNA Expression

Total RNA was purified from frozen muscles using TRIzol reagent (Invitrogen), according to manufacturer's instructions, treated with DNase, and reverse transcribed using Super Script II RNase H Reverse Transcriptase (Invitrogen) in the presence of Random Primers (Promega). Real-time PCR was performed using an ABI Prism 7900 apparatus (Applied Biosystems, Foster City, CA) at 60°C as the melting temperature, with the following primers: ribosomal protein large P0, 5′-CTCCAAGCAGATGCAGCAGA-3′ and 5′-ATAGCCTTGCGCATCATGG-3′; and Pax7 (paired-box gene 7), 5′-GGAAACCAGTGTGCCATCT-3′ and 5′-CCTTGTCTTTGGCACCATTT-3′.

Cell Transplantation

Quadruple-negative cells from WT and *Mtm1*δ4 donor mice cells were pelleted and resuspended in 1.2% barium chloride (Sigma Aldrich). The tibialis anterior (TA) muscles of isoflurane-anesthetized, 5- to 6-month-old C57BL/6 Rag1null *mdx*5cv mice were injected with a 10- to 15-μL suspension containing 50,000 cells. Mice were sacrificed 1 month after injection, and the TA muscles were frozen in isopentane for histological analysis. Cryosections (8-μm thick) were cut and stained for dystrophin (ab15277; Abcam) and DAPI at 80-μm intervals to evaluate dystrophin expression related to engraftment. Sections with the maximum number of positive fibers for a given muscle were photographed and counted. The maximum number of positive fibers in a given section was quantified for TA muscles injected with WT ($n = 4$) and KO ($n = 8$) cells, and compared using the Student's *t*-test. Additional cryosections (8-μm thick) were stained with H&E or Gomori trichrome to histologically evaluate the engraftment sites, as described later.

Cardiotoxin Injection

The right TA muscle of three isoflurane-anesthetized WT or *Mtm1*δ4 mice at 28 DOL were injected with 15- to 20-μL cardiotoxin (Sigma Aldrich) diluted at a final concentration of 0.5 μg/μL in sterile PBS. At 5 to 6 days after injection, the animals were euthanized and the TA muscles were extracted and snap frozen in isopentane.

Tissue Histological Data

Cross sections (8 μm thick) of isopentane–frozen TA or quadriceps muscle were taken midway down the length

of the muscle and stained with H&E and Gomori trichrome using standard techniques. IHC for Ki-67, a marker of cellular proliferation, was performed on TA muscles of cardiotoxin-injected animals by standard IHC techniques using Ki-67 primary antibody (ab16667; Abcam) and biotinylated horse anti-rabbit IgG (Vector Laboratories). TUNEL staining was performed on these muscles using an In Situ Cell Death Detection Kit POD (Roche, Indianapolis, IN), per the manufacturer's instructions. IHC for Pax7 was performed on TA muscles from cardiotoxin-injected animals and on quadriceps muscles from three uninjured WT and three *Mtm1*δ4 at 21 and 42 DOL after fixation of slides in 4% paraformaldehyde, blocking with both H_2O_2 and unconjugated Donkey Anti-Mouse IgG Fab Fragment (Jackson ImmunoResearch, West Grove, PA) in 1% bovine serum albumin, and exposure to Pax7 primary antibody (Developmental Studies Hybridoma Bank) and biotin-SP-conjugated donkey anti-mouse IgG Fab fragment (Jackson ImmunoResearch) secondary antibodies. Light microscopic images were captured using an Olympus DP72 camera and cellSens Standard software (Olympus, Center Valley, PA). Images were quantified by counting the number of positive cells within a field and dividing by the total number of fibers (for Pax7 and TUNEL) or nuclei (for Ki-67) within that field.

Results

To enrich for myogenic cells using FACS, our primary approach was to purify myogenic cells that were quadruple negative for SCA1, CD45, PDGFRα, and propidium iodide. SCA1 labeled most nonmyogenic cells in skeletal muscle,[19–21] although rare SCA1-expressing myogenic cells were also reported.[22–24] CD45 labeled immune cells, PDGFRα was a fibroadipogenic cell marker,[25,26] and propidium iodide was a marker of dead cells. Pooled limb muscles isolated from 26- to 30-day-old *Mtm1*δ4 mice and their WT male littermates consistently showed more quadruple-negative cells in *Mtm1*δ4 tissue ($P < 0.01$, $n = 5$), despite much higher tissue yields from the WT littermates (Figure 1A). Fusion assays revealed many desmin-expressing myoblasts and myotubes in both WT and *Mtm1*δ4 cultures, which confirmed that our sorting strategy enriched cultures for myogenic cells (Figure 1B). When areas of equivalent cellularity were quantified in WT and *Mtm1*δ4 myogenic cell cultures, the fusion index did not significantly vary between WT and *Mtm1*δ4 cultures (Figure 1B).

We further investigated the myogenic cell populations in *Mtm1*δ4 mice by evaluating the expression of Pax7, a marker of satellite cells, at the quiescent or early activated stage, in the quadruple-negative populations, and in isolated myofibers. When evaluating Pax7 expression per 200,000 cells, quadruple-negative *Mtm1*δ4 cells showed significantly decreased levels of Pax7 (36% ± 11% of WT values) expression (Figure 1C). Similarly, immunostaining for $Pax7^+$ satellite cells in cultured FDB fibers revealed that the number of $Pax7^+$ satellite cells in *Mtm1*δ4 FDBs (47.76 ± 10.0 fibers containing $Pax7^+$ cells per 100 fibers evaluated) was significantly lower

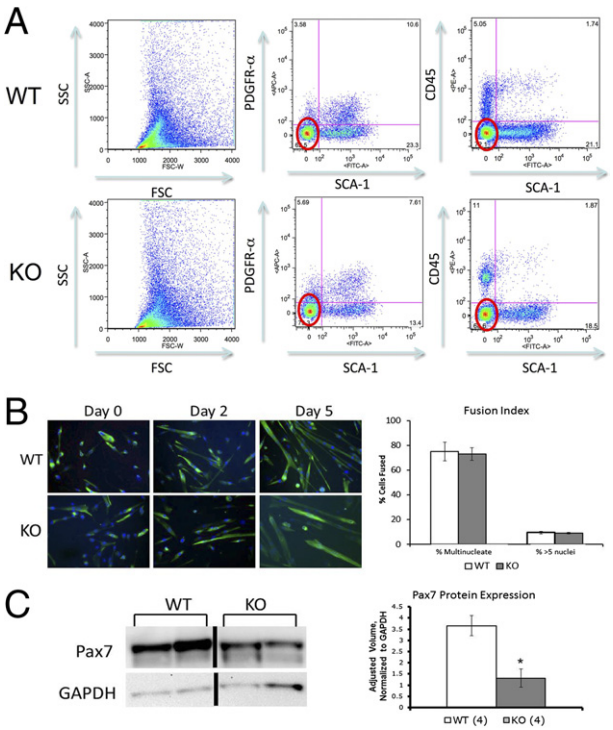

Figure 1. Properties of quadruple-negative cells. **A:** FACS of 25- to 30-day-old WT and *Mtm1*δ4 (KO) pooled limb muscles for $SCA1^-$, $PDGFR\alpha^-$, $CD45^-$, and propidium $iodide^-$ (ie, quadruple-negative) cells reveals that *Mtm1*δ4 mice possess significantly more quadruple-negative cells compared with WT littermates. $P < 0.01$. **B:** Immunostaining for desmin during a fusion assay confirms the myogenic potential of these cells and reveals similar fusion indices in equivalently populated regions of WT and *Mtm1*δ4 (KO) cell cultures. **C:** Western blot analyses performed on lysates of freshly sorted quadruple negative cells reveal decreased levels of Pax7 in *Mtm1*δ4 (KO) animals. $^*P < 0.05$. GAPDH, glyceraldehyde-3-phosphate dehydrogenase.

than in WT FDBs (78.62 ± 8.16 fibers containing $Pax7^+$ cells per 100 fibers evaluated) isolated from 26- to 30-day-old animals (Figure 2A). These findings suggested that the number of satellite cells in *Mtm1*δ4 animals was decreased compared with WT littermates, despite more quadruple-negative cells in *Mtm1*δ4 mice.

We further evaluated the number of prospective satellite cells in WT and *Mtm1*δ4 mice by using a different FACS strategy to isolate $CD31^-$, $CD45^-$, $CD106^+$ (Vcam-1) cells.[27] This strategy revealed that *Mtm1*δ4 animals at 45 to 49 DOL had significantly fewer Vcam-1^+ satellite cells compared with age-matched littermates (Figure 2B), further suggesting an age-related decrease in myogenic cells in *Mtm1*δ4 mice.

To evaluate the relationship between satellite cell number and progression of disease, Pax7 immunostaining was performed on quadriceps muscles from *Mtm1*δ4 animals at 21 and 42 DOL (Figure 3A). These studies detected significantly fewer satellite cells when comparing *Mtm1*δ4 muscle with age-matched WT animals. In addition, there was a significant decrease in the number of satellite cells found when comparing *Mtm1*δ4 animals at 21 and 42 DOL, confirming a marked decrease in the satellite cell population with the progression of disease. This finding was also confirmed through the evaluation of Pax7 mRNA levels at 14, 21, and 30 DOL in the *Mtm1*δ4 TA muscle (Figure 3B). Pax7 mRNA expression was de-

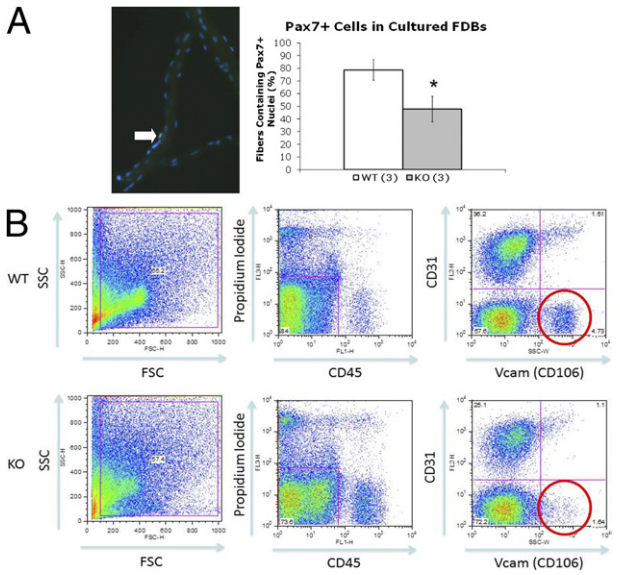

Figure 2. Decreased expression of Pax7 and number of prospective satellite cells are found in myotubularin-deficient muscle. **A:** Pax7 immunostaining of FDB fibers reveals fewer fibers containing $Pax7^+$ nuclei in myofibers isolated from *Mtm1*δ4 (KO) animals. $^*P < 0.05$. **B:** FACS of 45- to 49-day-old WT and *Mtm1*δ4 (KO) mouse muscle for $CD31^-CD45^-CD106^+$ ($Vcam1^+$ myogenic cells) reveals a depletion of this population in *Mtm1*δ4 muscle. $P < 0.05$. SSC, side scatter.

creased compared with WT values at 21 and 30 DOL. In addition, there was a significant decrease in Pax7 mRNA expression when comparing *Mtm1*δ4 animals at 14 and 30 DOL, consistent with the progression-related decrease in satellite cells observed in our IHC studies.

Although a decline in Pax7 expression was evident in *Mtm1*δ4 animals, quadruple-negative cells displayed myogenic activity *in vitro* and equal fusion capacity to WT cells. To determine whether myotubularin-deficient myogenic progenitors had the ability to function in a myotubularin-competent environment *in vivo*, we transplanted quadruple-negative cells from either *Mtm1*δ4 or WT mice at 25 to 30 DOL into the TA muscles of dystrophin-deficient C57BL/6 Rag1null *mdx*5cv mice and evaluated dystrophin expression 1 month after transplantation. Mdx5cv mice were used in this assay because they displayed approximately 10-fold less revertant fibers compared with *mdx* mice.[28] H&E and Gomori trichrome staining of implanted muscles showed no differences between muscles injected with WT or *Mtm1*δ4 cells. On IHC evaluation for dystrophin-positive fibers, which are an indicator of the successful engraftment of transplanted myogenic cells, *Mtm1*δ4 cells showed a dramatically decreased amount of engraftment (9.0 ± 3.8 dystrophin-positive fibers) compared with WT cells (38.5 ± 8.1 dystrophin-positive fibers), despite being transplanted at equivalent cell numbers (Figure 4A). Although this technique was unable to distinguish between engrafted and revertant fibers, there were fewer than nine dystrophin-positive fibers in six of the eight Mdx5cv muscles injected with *Mtm1*δ4 cells. These results suggested that the revertant fibers compose a minority of the dystrophin-positive fibers observed after the injection of Mdx5cv muscles with WT cells.

These engraftment findings suggested that *Mtm1*δ4 myogenic cells may be impaired with respect to survival and/or function. To address this, cell proliferation and apoptosis assays were performed. Quadruple-negative cells from 25- to 30-day-old *Mtm1*δ4 mice displayed decreased proliferation (51% to 70% of WT values, $P < 0.05$) immediately after sorting, but the difference in proliferation in WT and *Mtm1*δ4 animals was less pronounced (KO = 36% to 87% of WT values, P = ns) by 4 days after isolation (Figure 4B). Apoptosis after isolation was also measured using caspase-3 and caspase-7 activity, because abnormalities of the caspase apoptotic pathway and increased apoptosis were reported in myotubularin knockdown studies using HeLa cells.[9] Caspase-3 and caspase-7 activity was increased in *Mtm1*δ4 cells at 0, 2, and 4 days after isolation (178%, 151%, and 266% of WT levels, respectively; $P < 0.05$), consistent with persistently increased apoptosis in *Mtm1*δ4 myogenic cells (Figure 4C). Collectively, our find-

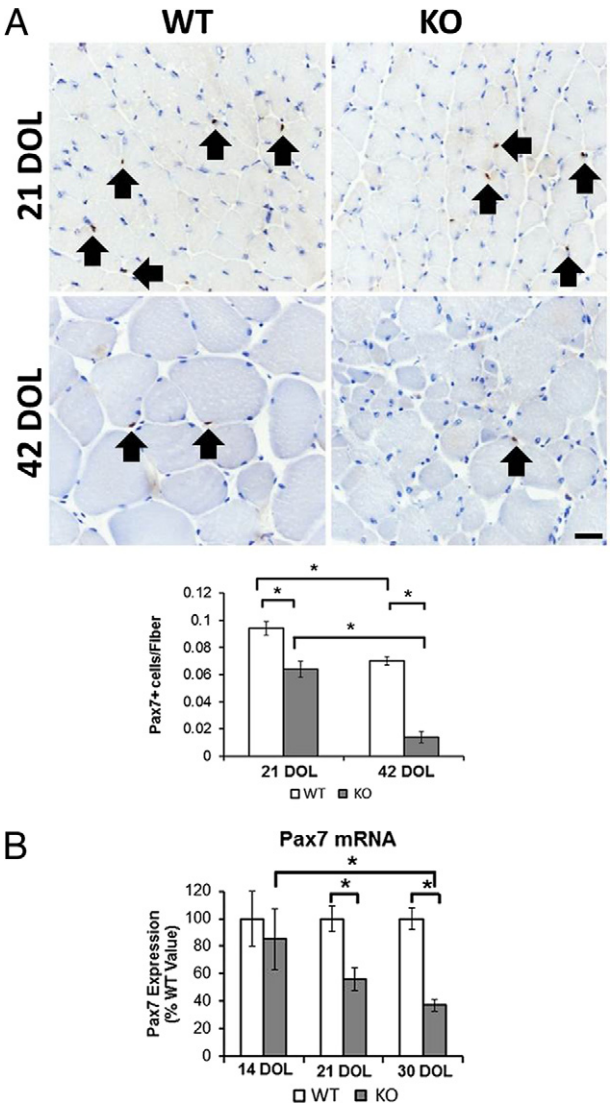

Figure 3. Depletion of satellite cells with progression of disease in *Mtm1*δ4 muscle. **A:** Immunostaining results for Pax7 in the quadriceps muscles of WT and *Mtm1*δ4 (KO) mice at 21 and 42 DOL are quantified to evaluate the satellite cell populations *in vivo*. **Arrows** indicate Pax7-positive nuclei in WT and KO animals. **B:** mRNA levels of 14-, 21-, and 30-day-old mice ($n = 9$) are quantified by quantitative RT-PCR, normalized to the ribosomal protein large P0 mRNA level, and compared with WT. Scale bar = 20 μm. $^*P < 0.05$.

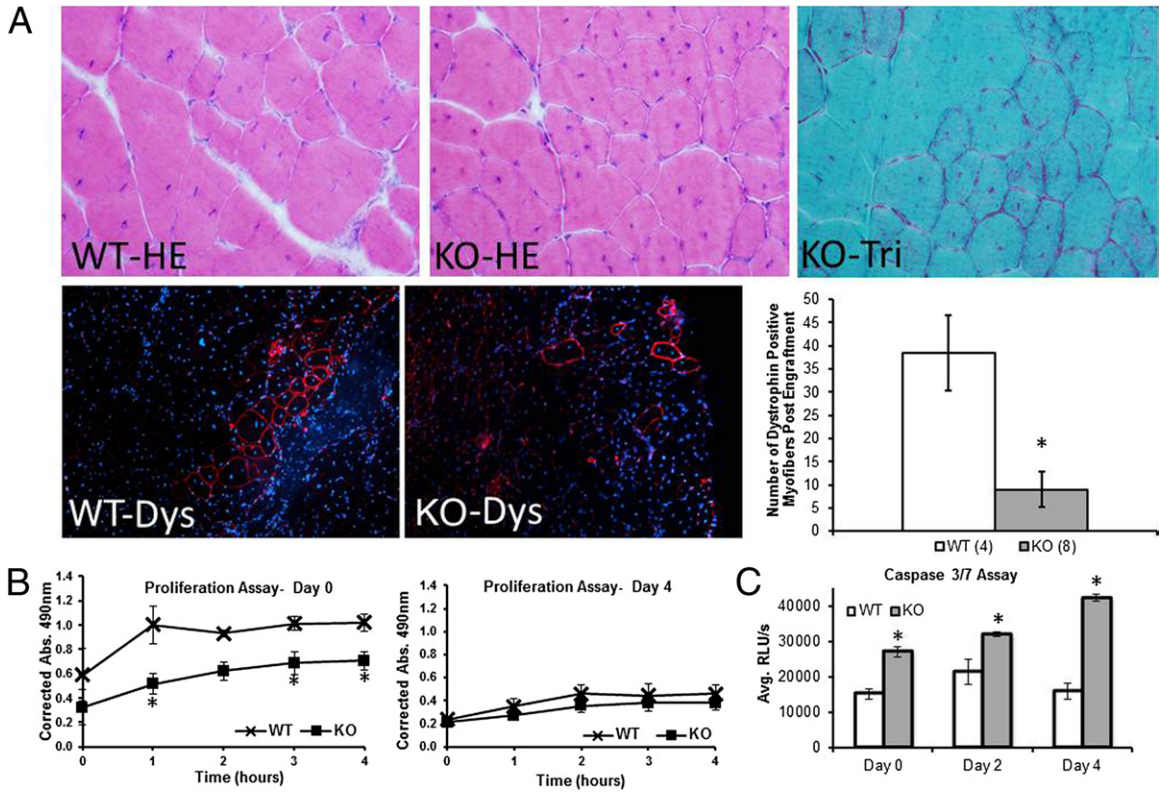

Figure 4. Poor survival of myotubularin-deficient cells *in vivo* and *vitro*. **A:** One month after transplantation of freshly sorted quadruple-negative cells into the TA muscles of C57BL/6 Rag1null *mdx*5cv mice, staining for dystrophin (Dys; red, **bottom panels**) and DAPI (blue) reveals significantly fewer successfully engrafted fibers after transplantation of *Mtm1*δ4 (KO) cells ($n = 8$) compared with WT cells ($n = 4$). $^*P < 0.01$. Quantification of dystrophin$^+$ fibers is performed by counting the highest number of dystrophin-expressing fibers within a single section of the entire TA muscle after surveying sections every 80 μm through the entire TA muscle. **Top panels:** H&E and trichrome stains of the injection site showing little or no fibrosis from the injected cells. **B:** Incorporation of MTS/PMS, which correlates with proliferation, is markedly higher in freshly isolated WT cells compared with cells from *Mtm1*δ4 (KO) littermates. There is no significant difference in proliferation after 4 days in culture. MTS, 3-(4,5-dimethylthiazol-2-yl)-5-(3-carboxymethoxyphenyl)-2-(4-sulfophenyl)-2H-tetrazolium, inner salt; PMS, phenazine methosulfate. **C:** A caspase-3/caspase-7 assay, which measures apoptosis through the activation of caspase-3/caspase-7, reveals increased caspase activation in *Mtm1*δ4 (KO) cells after FACS and at 2 and 4 days in culture. $^*P < 0.05$. Avg. RLU, relative light unit average.

ings indicated that the poor engraftment seen after transplantation of myoblasts from *Mtm1*δ4 mice was likely because of impairment of myogenic cell survival and proliferation, rather than abnormalities related to cell fusion.

The *in vivo* relevance of our findings was addressed through evaluation of the healing process and the baseline Pax7$^+$ satellite cell levels in *Mtm1*δ4 and WT mice. Five days after injection of the TA muscles of *Mtm1*δ4 mice with cardiotoxin, which produces a focal muscle injury and stimulates satellite cell activation, proliferation, and differentiation, *Mtm1*δ4 and WT muscle showed similar degrees of fiber regeneration and response to injury (Figure 5). Uninjured TA muscles showed pathological characteristics typical of myotubularin-deficient muscle, including marked fiber size variation and myofiber smallness in the absence of endomysial fibrosis, myonecrosis, or inflammation. Centrally nucleated fibers, which were less commonly seen in *Mtm1*δ4 mice, compared with other murine[29] and canine[30] models of myotubularin deficiency, were not significantly increased in the uninjured TA muscles at this time point (Figure 5). Regenerating areas in injured TA muscles were readily identifiable by the presence of numerous centrally nucleated fibers, surrounded by a mixed population of mononuclear cells composed of satellite cells, macrophages, and lymphocytes. Although mild fibrosis, interstitial edema, and an increase in the number of small blood vessels were noted on H&E and Gomori trichrome stains, these findings were present to an equivalent extent in regenerating WT and *Mtm1*δ4 muscles. On immunostaining for Pax7, Ki-67, and apoptotic cells (using a TUNEL assay), however, differences in the response to injury in WT and *Mtm1*δ4 mice became apparent. After injury, *Mtm1*δ4 muscle contained fewer satellite cells, fewer proliferative cells, and more apoptotic cells than WT muscle (Figure 5). Although not all of the proliferating and apoptotic cells might correspond to satellite cells, these data provided *in vivo* evidence for abnormal satellite cell behavior in *Mtm1*δ4 animals, involving abnormal levels of both proliferation and apoptosis.

Discussion

Several studies have been conducted on myotubularin-deficient cells in the past. Studies performed on myotubes from human patients reported normal cytoskeletal development, fusion, and behavior,[31,32] but proliferation, apoptosis, and engraftment were not evaluated. More recent work on *Mtm1*δ4 cells, cells with myotubularin knockdown, HeLa, and primary human cells, however, has revealed that myotubularin-deficient cells show abnormalities of cytoskeletal

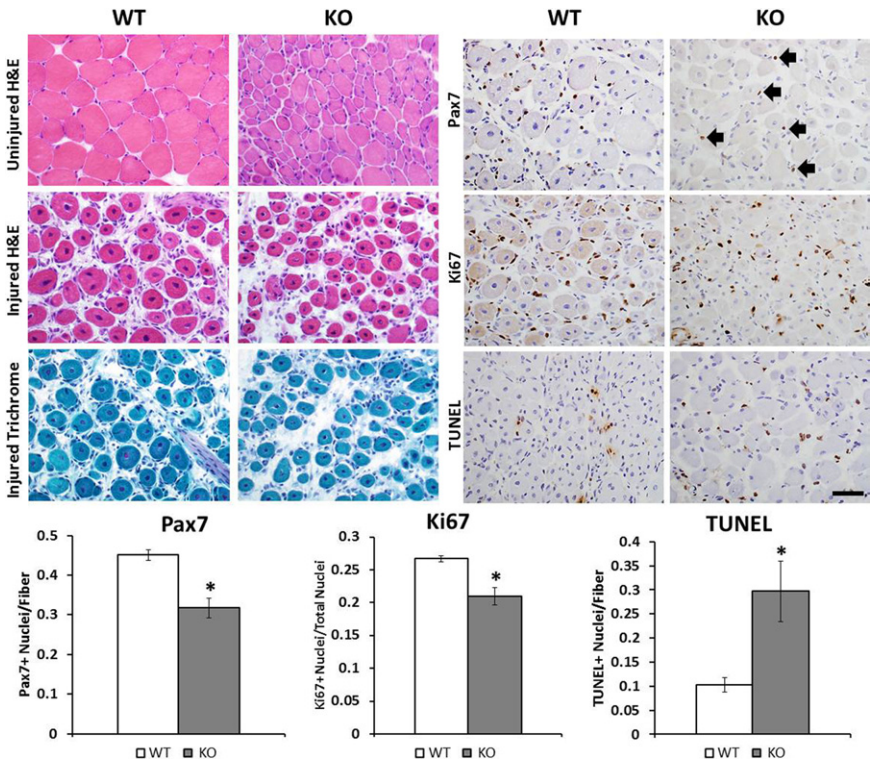

Figure 5. Reduced proliferation and increased apoptosis of myotubularin-deficient cells after injury. At 5 to 6 days after muscle injury by cardiotoxin, contralateral TA muscles from WT and *Mtm1δ4* (KO) mice show pathological features characteristic of uninjured muscle in these animals, including marked fiber size variation and marked myofiber smallness in *Mtm1δ4* muscles compared with WT. Injected TA muscles show signs of muscle regeneration, including numerous centrally nucleated myofibers, and the presence of a mixed population of mononuclear cells, mild fibrosis, and tissue edema (clear spaces) in the interstitial area between myofibers. IHC for satellite cells (Pax7), proliferating cells (Ki-67), and apoptotic cells (TUNEL) is also performed and quantified on regenerating muscles (**right panels**). **Arrows**, $Pax7^{+}$ satellite cells seen in regenerating *Mtm1δ4* muscle. Scale bar = 50 μm. $^{*}P < 0.05$.

organization[8] and intracellular signaling.[9] Although we were unable to detect abnormalities in desmin expression or cytoskeletal organization in cultured myoblasts and myotubes while staining for desmin in fusion assays, the techniques we used were not nearly as sensitive as those described by Hnia et al.[8] We were, however, able to demonstrate the presence of increased apoptosis in primary myotubularin-deficient myoblasts through increased activation of caspase-3 and caspase-7, consistent with the results reported in myotubularin-deficient cells.[9]

Abnormalities in the number and behavior of myogenic cells were also noted in *Mtm1δ4* muscle. Although there were more quadruple-negative cells in *Mtm1δ4* animals compared with WT littermates, further investigation by FACS, IHC, gene expression, and Western blot analysis revealed that Pax7 expression is consistently decreased when comparing *Mtm1δ4* with WT cell fractions and muscle tissue. In addition, data from these studies indicate that the number of myogenic cells markedly decreases with the progression of disease in *Mtm1δ4* mice. Our findings suggest that such depletion may occur through both slow proliferation and increased apoptosis of these myogenic cells. Depletion of satellite cells has been described in mice and humans deficient for dystrophin[33,34] and selenoprotein N[35] and in models of aging[36] and denervation.[37] Although this finding is nonspecific, it provides evidence for an additional degenerative component of the muscle dysfunction seen in myotubularin deficiency.

As an enzyme involved in sarcotubular and myofibrillar organization, endosomal trafficking, and excitation contraction coupling,[6–8] myotubularin may affect cell survival pathways through several mechanisms. Pathways involved in the induction of apoptosis include the activation of death receptors,[38] the release of apoptogenic factors from mitochondria,[39] and the unfolded protein response produced as the result of the accumulation of misfolded proteins in the endoplasmic reticulum.[40] Abnormalities in intracellular calcium produced in myotubularin deficiency[7] may cause mitochondrial stress and activation of the mitochondrial apoptotic pathway. Alternatively, abnormalities of sarcotubular organization may lead to the accumulation of proteins and induce the unfolded protein response. Further investigation is required to definitively identify the mechanism(s) by which myotubularin deficiency impairs satellite cell survival.

Because of the deficiency of a single, ubiquitously expressed enzyme that has been modeled in several animal systems, XLMTM is a disease with excellent potential for the development of successful treatment strategies. Significant limitations to the development or identification of potentially useful agents include the lack of a high-throughput *in vitro* assay on which new treatments could be tested and the difficulty in generating sufficient animals for preclinical trials on a rapid time scale. Although the relationship between the increased apoptosis and slowed proliferation in *Mtm1δ4* cells and the progression of disease in *Mtm1δ4* animals remains unclear, these cellular phenotypes represent reproducible phenotypes that can easily be tested in a high-throughput manner. The usefulness of myoblast cultures in evaluating novel treatment strategies will be studied as our laboratory continues to test novel agents in *Mtm1δ4* mice.

Acknowledgments

We thank Karine Poulard and Genethon's facilities for technical expertise.

References

1. Heckmatt JZ, Sewry CA, Hodes D, Dubowitz V: Congenital centronuclear (myotubular) myopathy: a clinical, pathological and genetic study in eight children. Brain 1985, 108(Pt 4):941–964
2. Jungbluth H, Wallgren-Pettersson C, Laporte J: Centronuclear (myotubular) myopathy. Orphanet J Rare Dis 2008, 3:26
3. Pierson CR, Tomczak K, Agrawal P, Moghadaszadeh B, Beggs AH: X-linked myotubular and centronuclear myopathies. J Neuropathol Exp Neurol 2005, 64:555–564
4. Tsujita K, Itoh T, Ijuin T, Yamamoto A, Shisheva A, Laporte J, Takenawa T: Myotubularin regulates the function of the late endosome through the gram domain-phosphatidylinositol 3,5-bisphosphate interaction. J Biol Chem 2004, 279:13817–13824
5. Buj-Bello A, Laugel V, Messaddeq N, Zahreddine H, Laporte J, Pellissier JF, Mandel JL: The lipid phosphatase myotubularin is essential for skeletal muscle maintenance but not for myogenesis in mice. Proc Natl Acad Sci U S A 2002, 99:15060–15065
6. Dowling JJ, Vreede AP, Low SE, Gibbs EM, Kuwada JY, Bonnemann CG, Feldman EL: Loss of myotubularin function results in T-tubule disorganization in zebrafish and human myotubular myopathy. PLoS Genet 2009, 5:e1000372
7. Al-Qusairi L, Weiss N, Toussaint A, Berbey C, Messaddeq N, Kretz C, Sanoudou D, Beggs AH, Allard B, Mandel JL, Laporte J, Jacquemond V, Buj-Bello A: T-tubule disorganization and defective excitation-contraction coupling in muscle fibers lacking myotubularin lipid phosphatase. Proc Natl Acad Sci U S A 2009, 106:18763–18768
8. Hnia K, Tronchere H, Tomczak KK, Amoasii L, Schultz P, Beggs AH, Payrastre B, Mandel JL, Laporte J: Myotubularin controls desmin intermediate filament architecture and mitochondrial dynamics in human and mouse skeletal muscle. J Clin Invest 2011, 121:70–85
9. Razidlo GL, Katafiasz D, Taylor GS: Myotubularin regulates Akt-dependent survival signaling via phosphatidylinositol 3-phosphate. J Biol Chem 2011, 286:20005–20019
10. Buj-Bello A, Fougerousse F, Schwab Y, Messaddeq N, Spehner D, Pierson CR, Durand M, Kretz C, Danos O, Douar AM, Beggs AH, Schultz P, Montus M, Denefle P, Mandel JL: AAV-mediated intramuscular delivery of myotubularin corrects the myotubular myopathy phenotype in targeted murine muscle and suggests a function in plasma membrane homeostasis. Hum Mol Genet 2008, 17:2132–2143
11. Lawlor MW, Read BP, Edelstein R, Yang N, Pierson CR, Stein MJ, Wermer-Colan A, Buj-Bello A, Lachey JL, Seehra JS, Beggs AH: Inhibition of activin receptor type IIb increases strength and lifespan in myotubularin-deficient mice. Am J Pathol 2011, 178:784–793
12. Buj-Bello A, Furling D, Tronchere H, Laporte J, Lerouge T, Butler-Browne GS, Mandel JL: Muscle-specific alternative splicing of myotubularin-related 1 gene is impaired in DM1 muscle cells. Hum Mol Genet 2002, 11:2297–2307
13. Gussoni E, Soneoka Y, Strickland CD, Buzney EA, Khan MK, Flint AF, Kunkel LM, Mulligan RC: Dystrophin expression in the mdx mouse restored by stem cell transplantation. Nature 1999, 401:390–394
14. Rando TA, Blau HM: Primary mouse myoblast purification, characterization, and transplantation for cell-mediated gene therapy. J Cell Biol 1994, 125:1275–1287
15. Qu-Petersen Z, Deasy B, Jankowski R, Ikezawa M, Cummins J, Pruchnic R, Mytinger J, Cao B, Gates C, Wernig A, Huard J: Identification of a novel population of muscle stem cells in mice: potential for muscle regeneration. J Cell Biol 2002, 157:851–864
16. Collins CA, Olsen I, Zammit PS, Heslop L, Petrie A, Partridge TA, Morgan JE: Stem cell function, self-renewal, and behavioral heterogeneity of cells from the adult muscle satellite cell niche. Cell 2005, 122:289–301
17. Shefer G, Yablonka-Reuveni Z: Isolation and culture of skeletal muscle myofibers as a means to analyze satellite cells. Methods Mol Biol 2005, 290:281–304
18. Wattanasirichaigoon D, Swoboda KJ, Takada F, Tong HQ, Lip V, Iannaccone ST, Wallgren-Pettersson C, Laing NG, Beggs AH: Mutations of the slow muscle alpha-tropomyosin gene, TPM3, are a rare cause of nemaline myopathy. Neurology 2002, 59:613–617
19. Sacco A, Doyonnas R, Kraft P, Vitorovic S, Blau HM: Self-renewal and expansion of single transplanted muscle stem cells. Nature 2008, 456:502–506
20. Sherwood RI, Christensen JL, Conboy IM, Conboy MJ, Rando TA, Weissman IL, Wagers AJ: Isolation of adult mouse myogenic progenitors: functional heterogeneity of cells within and engrafting skeletal muscle. Cell 2004, 119:543–554
21. Schulz TJ, Huang TL, Tran TT, Zhang H, Townsend KL, Shadrach JL, Cerletti M, McDougall LE, Giorgadze N, Tchkonia T, Schrier D, Falb D, Kirkland JL, Wagers AJ, Tseng YH: Identification of inducible brown adipocyte progenitors residing in skeletal muscle and white fat. Proc Natl Acad Sci U S A 2011, 108:143–148
22. Tamaki T, Akatsuka A, Ando K, Nakamura Y, Matsuzawa H, Hotta T, Roy RR, Edgerton VR: Identification of myogenic-endothelial progenitor cells in the interstitial spaces of skeletal muscle. J Cell Biol 2002, 157:571–577
23. Long KK, Montano M, Pavlath GK: Sca-1 is negatively regulated by TGF-beta1 in myogenic cells. FASEB J 2011, 25:1156–1165
24. Tanaka KK, Hall JK, Troy AA, Cornelison DD, Majka SM, Olwin BB: Syndecan-4-expressing muscle progenitor cells in the SP engraft as satellite cells during muscle regeneration. Cell Stem Cell 2009, 4:217–225
25. Joe AW, Yi L, Natarajan A, Le Grand F, So L, Wang J, Rudnicki MA, Rossi FM: Muscle injury activates resident fibro/adipogenic progenitors that facilitate myogenesis. Nature Cell Biol 2010, 12:153–163
26. Uezumi A, Fukada S, Yamamoto N, Takeda S, Tsuchida K: Mesenchymal progenitors distinct from satellite cells contribute to ectopic fat cell formation in skeletal muscle. Nature Cell Biol 2010, 12:143–152
27. Fukada S, Uezumi A, Ikemoto M, Masuda S, Segawa M, Tanimura N, Yamamoto H, Miyagoe-Suzuki Y, Takeda S: Molecular signature of quiescent satellite cells in adult skeletal muscle. Stem Cells 2007, 25:2448–2459
28. Danko I, Chapman V, Wolff JA: The frequency of revertants in mdx mouse genetic models for Duchenne muscular dystrophy. Pediatr Res 1992, 32:128–131
29. Pierson CR, Dulin-Smith AN, Durban AN, Marshall ML, Marshall JT, Snyder AD, Naiyer N, Gladman JT, Chandler DS, Lawlor MW, Buj-Bello A, Dowling JJ, Beggs AH: Modeling the human MTM1 p.R69C mutation in murine Mtm1 results in exon 4 skipping and a less severe myotubular myopathy phenotype. Hum Mol Genet 2012, 21:811–825
30. Beggs AH, Böhm J, Snead E, Kozlowski M, Maurer M, Minor K, Childers MK, Taylor SM, Hitte C, Mickelson JR, Guo LT, Mizisin AP, Buj-Bello A, Tiret L, Laporte J, Shelton GD: MTM1 mutation associated with X-linked myotubular myopathy in Labrador Retrievers. Proc Natl Acad Sci U S A 2010, 107:14697–14702
31. Van der Ven PF, Jap PH, Barth PG, Sengers RC, Ramaekers FC, Stadhouders AM: Abnormal expression of intermediate filament proteins in X-linked myotubular myopathy is not reproduced in vitro. Neuromuscul Disord 1995, 5:267–275
32. Dorchies OM, Laporte J, Wagner S, Hindelang C, Warter JM, Mandel JL, Poindron P: Normal innervation and differentiation of X-linked myotubular myopathy muscle cells in a nerve-muscle coculture system. Neuromuscul Disord 2001, 11:736–746
33. Blau HM, Webster C, Pavlath GK: Defective myoblasts identified in Duchenne muscular dystrophy. Proc Natl Acad Sci U S A 1983, 80:4856–4860
34. Webster C, Blau HM: Accelerated age-related decline in replicative life-span of Duchenne muscular dystrophy myoblasts: implications for cell and gene therapy. Somat Cell Mol Genet 1990, 16:557–565
35. Castets P, Bertrand AT, Beuvin M, Ferry A, Le Grand F, Castets M, Chazot G, Rederstorff M, Krol A, Lescure A, Romero NB, Guicheney P, Allamand V: Satellite cell loss and impaired muscle regeneration in selenoprotein N deficiency. Hum Mol Genet 2011, 20:694–704
36. Jejurikar SS, Henkelman EA, Cederna PS, Marcelo CL, Urbanchek MG, Kuzon WM Jr: Aging increases the susceptibility of skeletal muscle derived satellite cells to apoptosis. Exp Gerontol 2006, 41:828–836
37. Jejurikar SS, Marcelo CL, Kuzon WM Jr: Skeletal muscle denervation increases satellite cell susceptibility to apoptosis. Plast Reconstr Surg 2002, 110:160–168
38. Lavrik I, Golks A, Krammer PH: Death receptor signaling. J Cell Sci 2005, 118:265–267
39. Green DR: Apoptotic pathways: ten minutes to dead. Cell 2005, 121:671–674
40. Rasheva VI, Domingos PM: Cellular responses to endoplasmic reticulum stress and apoptosis. Apoptosis 2009, 14:996–1007